Offset Optimization in Signalized Traffic Networks via Semidefinite Relaxation

Samuel Coogan[a], Eric Kim[b], Gabriel Gomes[c], Murat Arcak[b], Pravin Varaiya[b]

[a] *Electrical Engineering Department, University of California, Los Angeles*
[b] *Department of Electrical Engineering and Computer Sciences, University of California, Berkeley*
[c] *Partners for Advanced Transportation Technology, University of California, Berkeley*

Abstract

We study the problem of selecting offsets of the traffic signals in a network of signalized intersections to reduce queues of vehicles at all intersections. The signals in the network have a common cycle time and a fixed timing plan. It is assumed that the exogenous demands are constant or periodic with the same period as the cycle time and the intersections are under-saturated. The resulting queuing processes are periodic. These periodic processes are approximated by sinusoids. The sinusoidal approximation leads to an analytical expression of the queue lengths at every intersection as a function of the demands and the vector of offsets. The optimum offset vector is the solution of a quadratically constrained quadratic program (QCQP), which is solved via its convex semidefinite relaxation. Unlike existing techniques, our approach accommodates networks with arbitrary topology and scales well with network size.

We illustrate the result in two case studies. The first is an academic example previously proposed in the literature, and the second case study consists of an arterial corridor network in Arcadia, California.

1. Introduction

Systematic approaches to selecting the parameters of traffic signal controllers—cycle time, green times, and intersection-to-intersection offsets—have been studied for several decades [1, 2]. Here we focus on the problem of selecting offsets for a network of signalized intersections to allow platoons of vehicles to move through the network with the least hindrance by red lights, a problem that has been considered at least since the development of SIGOP [3], one of the first computer programs for signal timing. In SIGOP, link delays are modeled as a parabolic function, and random simulations are used to determine incremental adjustments to signal offsets, which provides no guarantees of optimality. Many existing algorithms for offset optimization focus on one- or two-way arterial roads [4, 5]. Perhaps the first algorithm developed for general networks was the Combination Method [6, 7], in which link delay functions were combined into a network delay function using a set of network reduction rules. The method can be reformulated in terms of Dynamic Programming. As [6] notes, its computation and memory requirements grow rapidly. The mixed-integer formulation of the offset optimization problem was presented in [4], later generalized to grid networks in [8] by adding a "loop constraint", and further extended in [9] to provide computational advantages via a network decomposition technique. These methods suffer from the computational burden of mixed-integer programs and may not scale well. The approach in [5] optimizes offsets given a probability distribution of vehicle arrivals at each intersection but only considers two-way arterials and does not explicitly account for turning traffic.

In the offset optimization algorithms referenced above, the 'link delay function' or LDF of every link is given as part of the data. The LDF for a link ℓ is the delay (travel time over the link plus the queuing delay)

[☆] This work was supported in part by California Department of Transportation (Caltrans) and in part by NSF Grant CNS-1446145.

Email addresses: scoogan@ucla.edu (Samuel Coogan), eskim@eecs.berkeley.edu (Eric Kim), gomes@path.berkeley.edu (Gabriel Gomes), arcak@eecs.berkeley.edu (Murat Arcak), varaiya@eecs.berkeley.edu (Pravin Varaiya)

expressed as a function $\delta_\ell(\omega_\ell)$ of the relative offset ω_ℓ of the signals at the two ends of the link. It is assumed that this delay is independent of the relative offsets of all other links. Since the delay depends on the time profile of the vehicle flow over the link and since that profile in turn depends on the other offsets, it follows that $\delta_\ell(\omega_\ell)$ is a function only of the average link flow. For different levels of (average) demand, the delay will be different. An expression for the LDF assuming that the flow has the profile of a rectangular pulse is derived in [10]. Lastly, [11] derives expressions for the gradient of the delay based on the TRANSYT model for use in optimizing signal timing parameters, including offsets [12].

In this paper, we formulate the objective of the offset optimization problem as that of minimizing the queues at all intersections in the network, rather than of minimizing the sum of link delay functions. We approximate the flow of vehicles arriving at and departing from traffic signals as sinusoidal functions of time. The flows give rise to sinusoidal queues for which we derive closed-form analytical expressions. The problem of minimizing the average queue lengths at intersections is a non-convex, quadratically constrained quadratic program (QCQP) that is well-known to be amenable to semidefinite relaxation [13]. It seems to be a coincidence that this QCQP formulation and its relaxation are mathematically analogous to recent approaches to the optimal power flow problem [14] and the angular synchronization problem [15, 16].

We first apply our technique to an academic case study of a grid network with nine signalized intersections proposed in [10]. Based on simulations of the network, our optimization approach reduces mean peak queue length by 40.4% and reduces mean average queue length by 25.1% compared to parameters calculated in [10]. We then consider a case study arterial corridor network in Arcadia, California which is part of the Connected Corridors project at UC Berkeley [17]. The network contains thirteen signalized intersections, and simulation results show that our offset optimization technique reduces queue lengths by 27% and travel time by 8.9%. While these case studies are of modest size, the semidefinite formulation proposed here easily accommodates networks with up to approximately one hundred intersections.

The paper is organized as follows. Section 2 introduces notational preliminaries. Section 3 presents the problem formulation and Section 4 proposes an approach to modeling traffic flow and queue evolution using sinusoids. This approach leads to the offset optimization problem studied in Section 5. We consider two case studies in Section 6 and provide concluding remarks in Section 7. This paper significantly extends the results reported in the conference version [18] by formulating the model and our approach in the complex domain using phasor notation, which clarifies our main results, and also provides a second case study comparing our approach to previous results in the literature.

2. Preliminaries

We define $\mathbb{R}_{\geq 0} = \{x \in \mathbb{R} \mid x \geq 0\}$. For complex number $\mathbf{z} \in \mathbb{C}$, $\mathbf{z}^*$ is the complex conjugate of $\mathbf{z}$ and $\Re\{\mathbf{z}\}$ denotes the real part of $\mathbf{z}$. We denote the imaginary unit by i. For a matrix $M \in \mathbb{C}^{n\times m}$, $\mathbf{rank}(M)$ denotes the rank of M and M^H denotes the conjugate transpose of M. If M is square, then $\mathbf{Tr}(M)$ denotes the trace of M. If $M = M^H$ and $\mathbf{z}^H M\mathbf{z} \geq 0$ for all $\mathbf{z} \in \mathbb{C}^n$, then M is *positive semidefinite*, denoted by $M \succeq 0$. $M[j,k]$ denotes the (j,k)-th entry of M. For an index set $\mathcal{S}$, $\{x_s\}_{s\in\mathcal{S}}$ denotes a collection of elements indexed by $\mathcal{S}$. If $x_s \in \mathbb{R}$ or $x_s \in \mathbb{C}$ for each $s \in \mathcal{S}$, we identify $\{x_s\}_{s\in\mathcal{S}}$ with the vector $x \in \mathbb{R}^{|\mathcal{S}|}$ or $x \in \mathbb{C}^{|\mathcal{S}|}$ for some fixed enumeration of $\mathcal{S}$.

3. Problem Formulation

We consider a traffic network consisting of a set $\mathcal{S}$ of signalized intersections and a set $\mathcal{L}$ of *links*. A subset $\mathcal{E} \subset \mathcal{L}$ of links are *entry* links and direct exogenous traffic onto the network. The remaining links are *non-entry* links. Let $\sigma : \mathcal{L} \to \mathcal{S}$ map each link to the signal that serves the queue on that link, that is, $\sigma(\ell) = s \in \mathcal{S}$ if and only if signal s serves the queue on link ℓ. Symmetrically, let $\tau : \mathcal{L} \to \mathcal{S} \cup \epsilon$ map each link to the signal immediately upstream of the link where the symbol ϵ denotes that no upstream signal exists; that is, signal $\tau(\ell)$ controls the flow of vehicles to link ℓ and we have $\tau(\ell) = \epsilon$ if and only if $\ell \in \mathcal{E}$. See Figure 1 for an illustration of the notation. We emphasize that the network may contain loops.

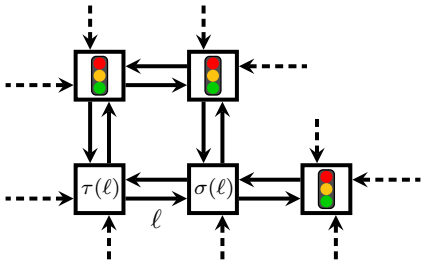

Figure 1: A standard network of signalized intersections along with the notation used. The nodes denote the intersections. For a link $\ell \in \mathcal{L}$, $\sigma(\ell)$ denotes the signal that serves ℓ and $\tau(\ell)$ denotes the signal immediately upstream of link ℓ. Entry links $\mathcal{E}$ are shown as dashed links. For all $\ell \in \mathcal{E}$, $\tau(\ell) = \epsilon$ where the symbol ϵ denotes the absence of an upstream signal. There is no need to model links that exit the network.

Parameter	Fraction of Cycle Time
Cycle time	$T = 1$
Phase offset of $s \in \mathcal{S}$	θ_s
Offset of arrival on $\ell \in \mathcal{L}$	φ_ℓ
Green split offset of $\ell \in \mathcal{L}$	γ_ℓ
Activation offset of $\ell \in \mathcal{L}$	$\theta_{\sigma(\ell)} + \gamma_\ell$
Queueing offset of $\ell \in \mathcal{L}$	ξ_ℓ
Travel time of $\ell \in \mathcal{L}$	λ_ℓ

Table 1: Parameters for the periodic, sinusoidal approximation of arrivals, departures, and queues.

Each signal at an intersection employs a *fixed time* control strategy whereby a repeating sequence of nonconflicting links are activated for a fixed amount of time. The length of time of this sequence is the *cycle time* of the intersection which we take to be 1 time unit:

Assumption 1 (Common Cycle Time)**.** *All signalized intersections have common cycle time* $T = 1$.

Table 1 collects notation for parameters introduced subsequently that arise from this fixed cycle time.

Each link $\ell \in \mathcal{L}$ possesses a queue with length $q_\ell(t) \in \mathbb{R}_{\geq 0}$ that evolves over time. We adopt a fluid queue model so that the queue length, arrivals, and departures are real-valued functions. Specifically, vehicles arrive at a queue from upstream links or from outside the network according to an arrival process $a_\ell(t)$ and depart the queue according to a departure process $d_\ell(t)$ which depends on the fixed time control of the signal. We describe how these processes are approximated under certain periodicity assumptions in Section 4. The queue length $q_\ell(t)$ then obeys the dynamics $\dot{q}_\ell(t) = a_\ell(t) - d_\ell(t)$. During a cycle, we assume that each link is activated for one contiguous interval of time (modulo a cycle length) during which vehicles depart the queue. For a signal $s \in \mathcal{S}$, the activation durations (*i.e.*, green times) for the upstream links $\{\ell \mid \sigma(\ell) = s\}$ and their sequencing are assumed to be fixed.

The *phase offset* $\theta_s \in [0, 1)$ for signal $s \in \mathcal{S}$ is the offset, as a fraction of the cycle length, of the activation sequence from some global clock and is the design parameter considered here. For each link $\ell \in \mathcal{L}$, let the *green split* $\gamma_\ell \leq [0, 1)$ be the time difference of the *midpoint* of the activation time for link ℓ and the beginning of the offset time $\theta_{\sigma(\ell)}$[1]. Here, we assume that the activation time includes the yellow time and any "all red" period. It follows that $t = n + (\theta_s + \gamma_\ell)$ for $n = 0, 1, 2, \ldots$ are the time instants of the midpoint of the activation times for each link ℓ with $\sigma(\ell) = s$. Define

$$\mathbf{z}_s = e^{i2\pi\theta_s} \quad \forall\ s \in \mathcal{L} \cup \epsilon \tag{1}$$

so that, instead of considering $\theta_s \in [0, 1)$, we equivalently consider $\mathbf{z}_s \in \mathbb{C}$ satisfying $|\mathbf{z}_s| = 1$. Without loss of generality, we interpret $\theta_\epsilon = 0$, that is, the offset of the entry links aligns with the global clock.

[1]We adopt a definition of green split that slightly differs from standard definitions by defining green split with respect to the midpoint of activation windows. Our motivation for doing so is that we seek to align the midpoints of the windows of green time from the upstream to downstream signal along each link to reduce queuing.

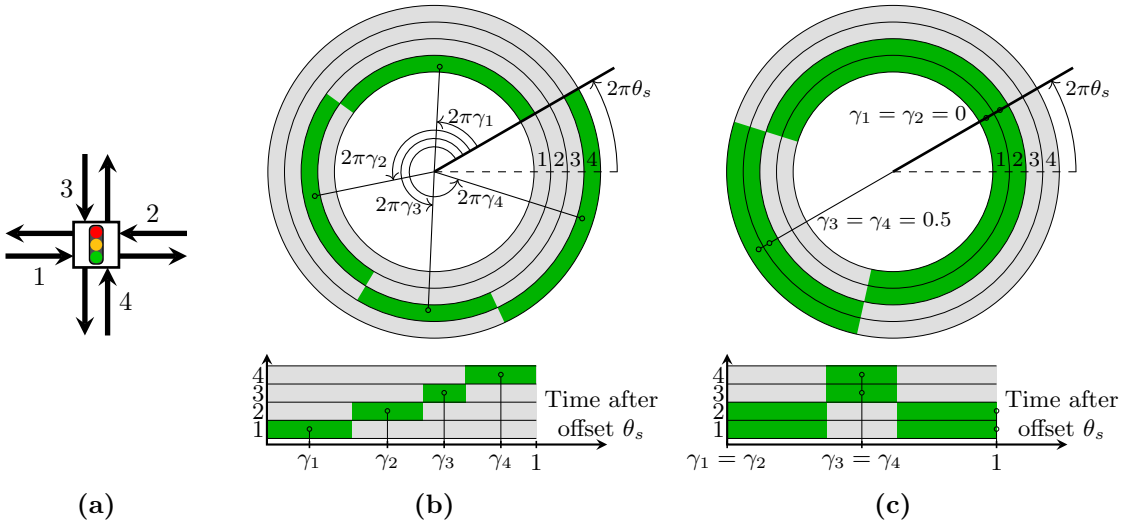

Figure 2: **(a)** A standard four-way intersection s with incoming links $1, 2, 3, 4$. The cycle time is divided among the incoming links according to the green splits at the intersection, which are assumed fixed. The phase offset $\theta_s \in [0, 1)$ for the intersection is a design parameter. **(b)** Green splits when each link is activated sequentially where time sweeps in a counter-clockwise direction, completing one rotation each cycle period (assumed to be $T = 1$). The green/dark regions denote the time intervals when a link is activated and queued vehicles are able to move through the intersection. **(c)** Green splits when links 1 and 2 are activated simultaneously, then links 3 and 4 are activated simultaneously. Without loss of generality, we take $\gamma_1 = \gamma_2 = 0$ and $\gamma_3 = \gamma_4 = 0.5$.

Example. *Consider signal $s \in \mathcal{S}$ with four input links $1, 2, 3,$ and 4 as in Figure 2(a). A possible set of green splits is shown in Figure 2(b). The green bands indicate the time interval, within one period, during which each link is activated. In the top image of Figure 2(b), one may imagine a line sweeping counter-clockwise at a rate of one revolution per cycle time $T = 1$ starting from the 0 angle. When this line reaches an angle of $2\pi\theta_s$, a new cycle begins at the intersection. The green portion of the innermost ring indicates when link 1 is activated, etc. This signaling pattern may be found in,* e.g.*, a four-way signaling scheme in which only one link is activated at any given time.*

Now suppose that links $\mathcal{L}^{pri} = \{1, 2\}$ are activated simultaneously during the primary *phase, and then links $\mathcal{L}^{sec} = \{3, 4\}$ are activated simultaneously during the* secondary *phase as in Figure2(c). This is a commonly encountered situation in which the signal consists of two phases for the two directions of travel. Without loss of generality, we assume that $\gamma_1 = \gamma_2 = 0$. An important observation for this common case is that, regardless of the length of the green splits, we have $\gamma_3 = \gamma_4 = 0.5$.*

For $\ell, k \in \mathcal{L}$, let the *turn ratio* $\beta_{\ell k} \in [0, 1]$ denote the fraction of vehicles that are routed to link k upon exiting link ℓ. We assume the turn ratios are given and fixed, a standard modeling assumption since turn ratios can be inferred from measured traffic flow [19]. Clearly, $\beta_{\ell k} \neq 0$ only if $\sigma(\ell) = \tau(k)$, and

$$\sum_{k \in \mathcal{L}} \beta_{\ell k} \leq 1 \quad \forall \ell \in \mathcal{L} \tag{2}$$

where strict inequality in (2) implies that a fraction of the vehicles departing link ℓ are routed off the network via an unmodeled link. We remark that our formulation is general enough to accommodate, *e.g.*, turn pocket lanes by introducing additional links for these lanes.

4. Sinusoidal Approximation of Arrivals, Departures, and Queues

To address the signal coordination problem discussed above, we assume the arrival and departure processes satisfy a periodicity assumption:

Assumption 2 (Periodicity Assumption)**.** *The network is in periodic steady state so that all arrivals, departures, and queues are periodic with period* $T = 1$*.*

The analysis of a standard queuing model of the network shows that if it is under-saturated under periodic exogenous arrivals with the same period as the cycle time, then the network converges to a periodic steady state [20]. Thus the Periodicity Assumption is reasonable. In our problem formulation we will approximate the arrival and departure processes at a queue as sinusoids of appropriate amplitude and phase shift. An enormous advantage of the sinusoidal approximation is that sinusoidal flows from several upstream links combine into a single sinusoidal flow with appropriate magnitude and phase.

In a related approach, Gartner and Deshpande rely on the Periodicity Assumption to calculate a Fourier series approximation to the assumed periodic link delay function based on simulated values for the link delay [21]. Here, we use the Periodicity Assumption to derive a tractable formulation of the offset optimization problem and then use simulation results to validate our approach.

4.1. Entry Links

For each $\ell \in \mathcal{E}$, we assume that the arrival of vehicles to the queue on link ℓ at signal $\sigma(\ell)$ is approximated by the function

$$a_\ell(t) = A_\ell + \alpha_\ell \cos(2\pi(t - \varphi_\ell)) \tag{3}$$

for constants A_ℓ and α_ℓ satisfying $0 \le \alpha_\ell \le A_\ell$ and $\varphi_\ell \in [0, 1)$. The constant A_ℓ is the average arrival rate of vehicles to the queue on link ℓ; α_ℓ allows for periodic fluctuation in the arrival rate; φ_ℓ is the offset of the periodic arrival of vehicles to the queue on link ℓ and includes the travel time of link ℓ. Define

$$\mathbf{a}_\ell = \alpha_\ell e^{-i2\pi\varphi_\ell} \tag{4}$$

so that, in phasor notation, $a_\ell(t) = A_\ell + \Re\{\mathbf{a}_\ell e^{i2\pi t}\}$.

When $A_\ell = \alpha_\ell$, $a_\ell(t)$ approximates a periodic pulse arrival, denoted by $\hat{a}_\ell(t)$ as in Figure 3(a), which is often used to model the arrival of vehicle platoons. If the periodic pulse has amplitude h_ℓ and duration δ_ℓ, we take $A_\ell = h_\ell\delta_\ell$ so that $\int_0^1 a_\ell(t)dt = \int_0^1 \hat{a}_\ell(t)dt = h_\ell\delta_\ell$. In this case, φ_ℓ is the midpoint of the arrival pulse.

The departure process $d_\ell(t)$ for entry link $\ell \in \mathcal{E}$ is determined by the signal at intersection $\sigma(\ell) \in \mathcal{S}$ and must satisfy $\int_0^1 d_\ell(t)\ dt = \int_0^1 a_\ell(t)\ dt$ by the Periodicity Assumption. We approximate the departure process as a shifted sinusoid so that, for all $\ell \in \mathcal{E}$,

$$\begin{aligned} d_\ell(t) &= A_\ell\big(1 + \cos(2\pi[t - (\theta_{\sigma(\ell)} + \gamma_\ell)])\big) &(5)\\ &= A_\ell + \Re\{\mathbf{d}_\ell \mathbf{z}^*_{\sigma(\ell)} e^{i2\pi t}\} &(6)\end{aligned}$$

for $\mathbf{d}_\ell := A_\ell e^{-i2\pi\gamma_\ell}$ where, as defined above, $(\theta_{\sigma(\ell)} + \gamma_\ell)$ denotes the activation offset of link ℓ as determined by the phase offset of signal $\sigma(\ell)$ and the green split of link ℓ; see Figure 3(b). We assume that all links have adequate capacity for upstream traffic and thus do not consider blocking of traffic by downstream congestion.

4.2. Non-entry Links

For each link $\ell \in \mathcal{L}\backslash\mathcal{E}$, let λ_ℓ denote the travel time of link ℓ, that is, the time it takes for a vehicle to travel along a link and join a downstream queue. We adopt a *vertical queueing* model as in [10, 22] and therefore assume the travel time is constant. When the link length is long as compared to the average queue length, this is a reasonable approximation. The approximate arrival process for the queue on link $\ell \in \mathcal{L}\backslash\mathcal{E}$ is then

$$a_\ell(t) = \sum_{k \in \mathcal{L}} \beta_{k\ell} d_k(t - \lambda_\ell) = A_\ell + \Re\{\mathbf{a}_\ell \mathbf{z}^*_{\tau(\ell)} e^{i2\pi t}\} \tag{7}$$

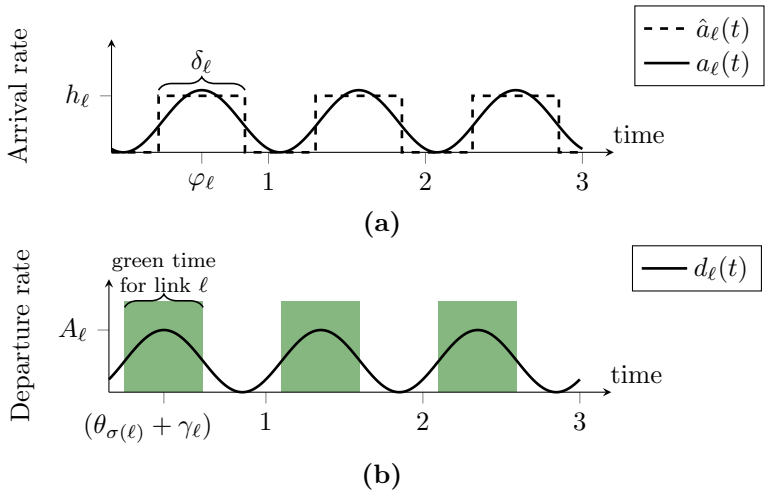

Figure 3: Sinusoidal approximations of arrivals and departures. **(a)** A particular approximation of the arrival process on an entry link. The actual arrival process for link $\ell \in \mathcal{E}$ is a pulse train, which is approximated with a sinusoid. **(b)** The sinusoidal approximation of the departure process at any link $\ell \in \mathcal{L}$. The amplitude is required to match A_ℓ by the Periodicity Assumption, and the phase offset $\theta_{\sigma(\ell)}$ is a design parameter.

where

$$A_\ell = \sum_{k \in \mathcal{L}} \beta_{k\ell} A_k \tag{8}$$

$$\mathbf{a}_\ell = e^{-i2\pi\lambda_\ell} \sum_{k \in \mathcal{L}} \beta_{k\ell} \mathbf{d}_\ell =: \alpha_\ell e^{-i2\pi\varphi_\ell}. \tag{9}$$

In (7), we use the fact that $\sigma(k) = \tau(\ell)$ for any k, ℓ such that $\beta_{k\ell} \neq 0$, and in (9), we define α_ℓ and φ_ℓ so that $\mathbf{a}_\ell = \alpha_\ell e^{-i2\pi\varphi_\ell}$. Because the departure processes at upstream links are assumed sinusoidal with period T, we obtain a sinusoidal arrival process with period T as seen in (7) that naturally and implicitly accounts for traffic arriving from multiple upstream movements, *e.g.*, through movements and turning movements. The combined effects of vehicle platoons departing from multiple movements arriving on link ℓ are therefore captured in the parameters A_ℓ and $\mathbf{a}_\ell$.

Under the periodicity assumption, the actual arrival and departure processes are periodic. By approximating arrivals and departures as sinusoids, we may interpret our approach as considering only the fundamental harmonic of the true processes. This is a natural formulation for the offset optimization problem because there is only one variable to tune at each intersection, namely, the intersection's offset.

The approximate departure process for each non-entry link $\ell \in \mathcal{L} \backslash \mathcal{E}$ is as described above for entry links. In summary, for each link $\ell \in \mathcal{L}$, we approximate the arrival and departure process as

$$d_\ell(t) = A_\ell + \Re\{\mathbf{d}_\ell \mathbf{z}^*_{\sigma(\ell)} e^{i2\pi t}\}, \qquad \mathbf{d}_\ell = A_\ell e^{-i2\pi\gamma_\ell} \tag{10}$$

$$a_\ell(t) = A_\ell + \Re\{\mathbf{a}_\ell \mathbf{z}^*_{\tau(\ell)} e^{i2\pi t}\}, \qquad \mathbf{a}_\ell = \alpha_\ell e^{-i2\pi\varphi_\ell} \tag{11}$$

where A_ℓ, α_ℓ, γ_ℓ, and φ_ℓ do not depend on the offsets $\{\theta_s\}_{s \in \mathcal{S}}$, that is, $\mathbf{a}_\ell$ and $\mathbf{d}_\ell$ are fixed quantities obtained from the problem data independent of the optimization variables $\mathbf{z}_s$ for $s \in \mathcal{S}$.

4.3. Queueing Process

The approximate queueing process $q(t)$ that results from the sinusoidal approximation of arrivals and departures satisfies

$$\dot{q}_\ell(t) = a_\ell(t) - d_\ell(t) = \Re\{(\mathbf{a}_\ell \mathbf{z}^*_{\tau(\ell)} - \mathbf{d}_\ell \mathbf{z}^*_{\sigma(\ell)}) e^{i2\pi t}\} = Q_\ell \cos(2\pi(t - \xi_\ell)) \tag{12}$$

where

$$Q_\ell^2 = \left|\mathbf{a}_\ell \mathbf{z}_{\tau(\ell)}^* - \mathbf{d}_\ell \mathbf{z}_{\sigma(\ell)}^*\right| = A_\ell^2 + \alpha_\ell^2 - 2A_\ell\alpha_\ell \cos(2\pi(\theta_{\tau(\ell)} + \varphi_\ell) - 2\pi(\theta_{\sigma(\ell)} + \gamma_\ell)) \tag{13}$$

and ξ_ℓ is the offset of the queueing process; here, we do not require an explicit expression for ξ_ℓ. It follows by integration that $q_\ell(t) = \frac{1}{2\pi} Q_\ell \sin(2\pi(t - \xi_\ell)) + C_\ell$ where C_ℓ is the average queue length on link ℓ. Under the assumption that all queues are emptied in each cycle, which is the case if the demand is *strictly feasible* [20, 22], we have $C_\ell = Q_\ell/(2\pi)$.

4.4. Performance Metric

For link $\ell \in \mathcal{L}$, consider the performance metric $J_\ell \triangleq Q_\ell^2$. J_ℓ is an approximate measure of the squared average queue length on link ℓ and the maximum squared queue length on link ℓ up to a constant factor. Since A_ℓ, α_ℓ do not depend on the signal offsets, minimizing J_ℓ is equivalent to maximizing the normalized reward function

$$R_\ell = A_\ell\alpha_\ell \cos(2\pi(\theta_{\tau(\ell)} + \varphi_\ell) - 2\pi(\theta_{\sigma(\ell)} + \gamma_\ell)) \tag{14}$$

$$= \Re\{\mathbf{d}_\ell \mathbf{a}_\ell^* \mathbf{z}_{\tau(\ell)} \mathbf{z}_{\sigma(\ell)}^*\}. \tag{15}$$

The interpretation of maximizing R_ℓ is clear: for each link, we wish to minimize the difference between the arrival offset $(\theta_{\tau(\ell)} + \varphi_\ell)$ and the departure offset $(\theta_{\sigma(\ell)} + \gamma_\ell)$. Choosing $\theta_{\sigma(\ell)} + \gamma_\ell = \theta_{\tau(\ell)} + \varphi_\ell$ optimizes the offset of signals $\sigma(\ell)$ and $\tau(\ell)$ from the perspective of reducing the queue length on link ℓ; the difficulty arises in choosing the offsets for all signals simultaneously, as it is generally not possible to maximize R_ℓ for all $\ell \in \mathcal{L}$. Efficiently computing an optimal tradeoff is addressed in the next section.

5. Optimizing Traffic Signal Offsets

5.1. Offset optimization problem and a convex relaxation

We propose $\sum_{\ell\in\mathcal{L}} R_\ell$ as the global objective function for the network and thus pose the following by substituting (14):

Offset Optimization Problem:

$$\underset{\mathbf{z}_s\in\mathbb{C},\ s\in\mathcal{S}\cup\epsilon}{\text{maximize}} \qquad \sum_{\ell\in\mathcal{L}} \Re\{\mathbf{d}_\ell \mathbf{a}_\ell^* \mathbf{z}_{\tau(\ell)} \mathbf{z}_{\sigma(\ell)}^*\} \tag{16}$$

$$\text{subject to} \qquad |\mathbf{z}_s| = 1 \quad \text{for all } s \in \mathcal{S} \cup \epsilon. \tag{17}$$

The constraint $|\mathbf{z}_s| = 1$ ensures there exists offset θ_s such that $\mathbf{z}_s = e^{i2\pi\theta_s}$, thus optimizing over $\mathbf{z}_s$ for $s \in \mathcal{S}$ subject to $|\mathbf{z}_s| = 1$ is equivalent to optimizing over the offset variables $\theta_s \in [0, 1)$ for $s \in \mathcal{S}$. In Sections 3 and 4, we have assumed $\theta_\epsilon = 0$. Here, we include θ_ϵ as a decision variable in the optimization problem for convenience; this is clearly acceptable since the objective function in (16) is invariant to a shift of all θ_s, $s \in \mathcal{S} \cup \epsilon$. In particular, given a solution to (16), we may shift all phases by the nonzero θ_ϵ to obtain an alternative solution as is done below in (23)[2].

The optimization problem (16)–(17) is a quadratically constrained, quadratic optimization problem (QCQP). To see this, let[3] $\mathcal{L}_{s\to u} = \{\ell \in \mathcal{L} \mid \tau(\ell) = s \text{ and } \sigma(\ell) = u\}$ be the set of links connecting intersection s to u and define $W \in \mathbb{C}^{(|\mathcal{S}|+1)\times(|\mathcal{S}|+1)}$ elementwise as follows:

$$W[u, s] = \frac{1}{2}\left(\sum_{\ell\in\mathcal{L}_{s\to u}} \mathbf{d}_\ell \mathbf{a}_\ell^* + \sum_{\ell\in\mathcal{L}_{u\to s}} \mathbf{d}_\ell^* \mathbf{a}_\ell\right). \tag{18}$$

[2]Note that the "loop constraint", which requires the sum of offset differences along any cycle in the network to sum to an integer multiple of the cycle time [8], is automatically satisfied by our choice of $\mathbf{z}$.

[3]The set $\mathcal{L}_{s\to u}$ may have cardinality greater than one if, *e.g.*, we model turn pocket lanes with additional links as remarked above.

Note that W is Hermitian, that is, $W = W^H$. Let $\mathbf{z} = \{\mathbf{z}_s\}_{s\in\mathcal{S}\cup\epsilon}$ so that

$$\sum_{\ell\in\mathcal{L}} \Re\{\mathbf{d}_\ell \mathbf{a}_\ell^* \mathbf{z}_{\tau(\ell)} \mathbf{z}_{\sigma(\ell)}^*\} = \mathbf{z}^H W \mathbf{z}. \tag{19}$$

In general, the QCQP in (16)–(17) is not convex; the nonconvexity arises from both the cost function $\mathbf{z}^H W\mathbf{z}$ and the constraints $|\mathbf{z}_s| = 1$ which can be written as $\mathbf{z}^H M_s \mathbf{z} = 1$ where $M_s \in \mathbb{C}^{(|\mathcal{S}|+1)\times(|\mathcal{S}|+1)}$ and satisfies $M_s[s,s] = 1$ and $M_s[s,u] = 0$ for $s \neq u$.

Here, we suggest a standard relaxation for approximately solving (16) using invariance of the trace operator under cyclic permutations so that $\mathbf{z}^H W\mathbf{z} = \mathbf{Tr}(\mathbf{z}^H W\mathbf{z}) = \mathbf{Tr}(W\mathbf{z}\mathbf{z}^H)$. We thus consider the following convex, semidefinite program (SDP) over $\mathbf{Z} \in \mathbb{C}^{(|\mathcal{S}|+1)\times(|\mathcal{S}|+1)}$:

$$\begin{aligned} \underset{\mathbf{Z}}{\text{maximize}} \quad & \mathbf{Tr}(W\mathbf{Z}) && (20)\\ \text{subject to} \quad & \mathbf{Z}[s,s] = 1, \quad s \in \mathcal{S}\cup\epsilon && (21)\\ & \mathbf{Z} \succeq 0 && (22) \end{aligned}$$

A positive semidefinite matrix $\mathbf{Z}$ is factorable as $\mathbf{Z} = \mathbf{z}\mathbf{z}^H$ if and only if $\mathbf{rank}(\mathbf{Z}) = 1$. Thus, a solution $\mathbf{Z}_\star$ of (20)–(22) provides a solution $\mathbf{z}_\star$ to (16)–(17) for which $\mathbf{Z}^\star = \mathbf{z}_\star(\mathbf{z}_\star)^H$ if and only if $\mathbf{rank}(\mathbf{Z}_\star) = 1$. There exist known cases for which this condition holds. For example, it is known that certain sparsity structure in W implies $\mathbf{rank}(\mathbf{Z}_\star) = 1$ and therefore leads to exact recovery of an optimal solution [23]. Sparsity in W translates to topological requirements on the traffic network. For instance, if the sparsity structure in W corresponds to a tree graph, then there exists a rank-one solution to (20)–(22) [23]. In traffic networks, a tree structure means that there are no cycles in the undirected network obtained by ignoring the directionality of the traffic flow and removing duplicate links between intersections.

Furthermore, for cases when the optimal $\mathbf{Z}_\star$ is not rank-one, there exists randomized techniques for obtaining a feasible solution to (16)–(17) that is guaranteed to be close to optimal in expectation. For example, [24] proposes a technique for estimating a solution based on the Cholesky factorization of $\mathbf{Z}_\star$.

Remarkably, for many problems of practical interest, it has been empirically observed that there exists a rank-one solution to (20)–(22) even in cases which are not known to guarantee this rank condition [15], and thus we obtain an optimal solution to the offset optimization problem. In both case studies below, we obtain a solution that is rank-one and therefore exactly recover an optimal solution to the original offset optimization problem in (16)–(17).

Let $\mathbf{z}_\star = \{\mathbf{z}_{\star s}\}_{s\in\mathcal{S}\cup\epsilon}$ be the result of solving (20)–(22) obtained either as an exact solution to (16)–(17) if $\mathbf{Z}_\star$ is rank-one or as an approximate solution otherwise. Then we obtain intersection offsets as

$$\theta_s = \frac{1}{2\pi}(\angle\mathbf{z}_{\star s} - \angle\mathbf{z}_{\star\epsilon}) \tag{23}$$

where $\angle$ denotes angle (in radians) in the complex plane.

If there exists $s \in \mathcal{S}\cup\epsilon$ such that $W[s,u] = W[u,s] = 0$ for all $u \in \mathcal{S}$, then $\mathbf{z}_s$ does not appear in the objective of (16) and the decision variables $\mathbf{z}_s$ may be removed from the optimization problem prior to the convex relaxation. For example, if $\alpha_\ell = 0$ for all $\ell \in \mathcal{E}$, as is in the case studies below where vehicles are assumed to arrive at entry links as a steady stream, then $\mathbf{z}_\epsilon$ may be removed from the optimization problem and we can arbitrarily take $\angle\mathbf{z}_{\star\epsilon} = 0$ in (23).

6. Case Studies

We provide two case studies. The first case study considers the grid network proposed in [10], and we compare our results to those reported there. The second case study considers a real arterial corridor in Arcadia, California.

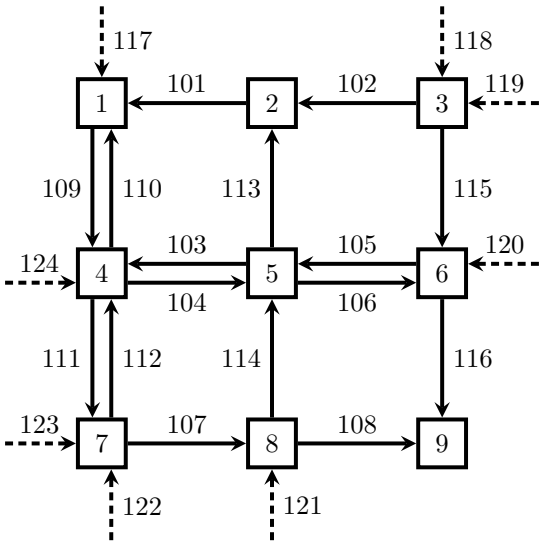

Figure 4: Grid network case study with 9 intersections, 8 entry links, and 16 non-entry links as proposed in [10].

Link ID	Flow [veh/sec]
117	0.175
118	0.175
119	0.152
120	0.152
121	0.12
122	0.11
123	0.25
124	0.22

Table 2: Incoming flow for grid network. All traffic is assume to travel straight through intersections so that there are no left or right turns.

6.1. Grid Network

We first consider the grid network shown in Figure 4. This example appears in [10] and consists of 9 intersection, 8 entry links, and 16 non-entry links. In [10], it is assumed that all traffic moves straight at intersections and there are no turns, and we adopt the same assumption here in order for our results to be comparable to those reported in [10]. We note that our methodology would apply without any modification to the case with turning traffic. Table 2 contains the traffic flow at the entry links. In [10], the offsets are optimized using a mixed integer formulation with the goal of minimizing a weighted sum of *link performance functions* which is intended to capture the average delay per vehicle in the network. The performance function is approximated with a piecewise linear function, and the mixed integer optimization framework implies that the methodology does not scale well. Here, we compare the results reported in [10] with results obtained using the offset optimization scheme proposed above.

As it is assumed that traffic at the entry links arrives at the network in a steady stream, we have that $\alpha_\ell = 0$ for all $\ell \in \mathcal{E}$, and A_ℓ is equal to the average flow in Table 2. We thus omit $\mathbf{z}_\epsilon$ from the optimization problem as remarked above. The cycle time of the network is 80 seconds.

We solve the convex semidefinite optimization problem (20)–(22) using the python package CVXOPT [25] which returns an optimal $\mathbf{Z}_\star$ in 27.4 milliseconds on a standard laptop. For this case study, CVXOPT returned $\mathbf{Z}_\star$ such that $\mathbf{rank}(\mathbf{Z}_\star) = 1$, that is, we are able to obtain a global solution to the original nonconvex problem (16)–(17) by factoring $\mathbf{Z}_\star = \mathbf{z}_\star(\mathbf{z}_\star)^H$. This solution is optimal with respect to the performance

Link ID	Travel Time	Link Offset [sec]		Peak Queue [veh]		Average Queue [veh]	
	[sec]	Gartner	SDP	Gartner	SDP	Gartner	SDP
101	18.59	21.2	17.3	3	2	0.77	0.61
102	24.79	27.6	26.4	3	2	0.75	0.62
103	18.59	63.6	69.3	13	12	6.69	6.70
104	14.61	16.4	10.7	2	2	0.68	0.68
105	24.79	46.4	59.6	11	13	3.21	5.15
106	19.48	33.6	20.4	14	2	2.99	0.67
107	14.61	17.2	13.6	2	2	0.83	0.83
108	19.48	25.2	21.2	5	2	1.64	0.82
109	28.41	23.6	32.4	2	4	1.04	1.16
110	24.35	56.4	47.6	9	3	3.28	0.92
111	15.62	28.4	8.2	9	3	2.81	1.67
112	13.39	51.6	71.8	9	3	3.70	1.16
113	24.35	18.8[a]	19.6	2	2	0.77	1.14
114	13.39	50.8[a]	68.9	10	6	4.04	2.91
115	28.41	42.4	27.2	10	4	2.73	1.61
116	15.62	20.8	12.0	5	3	1.85	1.67
			Mean	6.81	4.06	2.36	1.77
			Improvement	**40.4%**		**25.1%**	

[a]The collection of link offsets reported in [10] is not physically realizable, that is, there does not exist a set of intersection offsets that gives rise to all of the specified offsets simultaneously. To correct this error, we report slightly modified link offsets for links 113 and 114 that result in a realizable collection of link offsets.

Table 3: Results for grid network case study and comparison to results obtained in [10].

metric and cost function defined in (14)–(17). SDP solvers such as CVXOPT use standard interior point algorithms to obtain the optimal solution in polynomial time.

In Table 3, we report the results of our optimization and compare to the results in [10]. Because each link receives flow upstream from only one link, it is possible to define a *link offset* that is the difference between the time of activation of a link at an intersection and the time of activation for the same direction of traffic at the upstream link. We measure link offset with respect to the midpoint of the green times at each intersection. In [10], the link offset is measured with respect to the beginning of the green time, thus the link offsets in Table 3 for "Gartner" differ from the numbers in [10] but represent the same collection of signal offsets. The green times for each link are found in [10]. To obtain good traffic progression, we desire the link offsets to be close to the travel times for each link.

To compare our results with the results in [10], we simulate the network using the PointQ simulator [26], a mesoscopic simulation environment developed at UC Berkeley. The simulator is event driven and models individual vehicles in the network. In the simulation, each vehicle travels along the links and joins finite capacity queues at intersections. If a link's capacity is exceeded, the vehicle is held at the preceding queue, and thus our simulator captures queue spillback effects. In addition, vehicles move through intersections at a specified saturation rate when queues are served. For this case study, we use the saturation rates and green times reported in [10]. The interarrival time for vehicles at entry links is determined by the flows in Table 2.

In Table 3, we report the link offset, peak queue length, and average queue length for each non-entry link in the network using the offsets from [10] under the heading "Gartner" and using the offsets obtained with our optimization strategy under the heading "SDP". Note that, because vehicles arrive as a steady stream at entry links, the peak and average queues of entry links are unaffected by the choice of offsets. The offset optimization approach proposed in this paper improves the mean peak queue by 40.4% and the mean average queue by 25.1%.

By adopting the assumptions in [10], we are able to compare our results to those in the literature, however

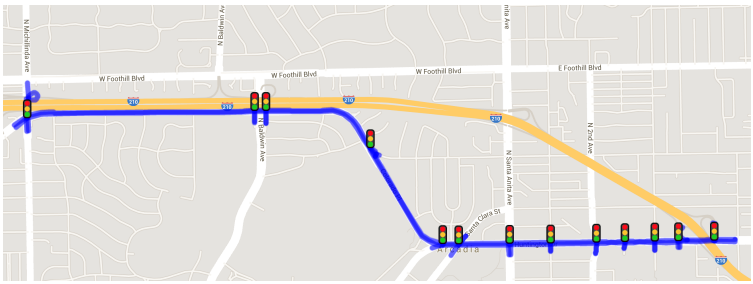

Figure 5: Huntington Dr./Colorado Blvd. arterial corridor in Arcadia, California. The case study consists of 50 links and 13 signalized intersections.

these assumptions are restrictive. In the next case study, we consider an actual traffic network for which real data are available.

6.2. Arterial Corridor in Arcadia, California

We next consider the Huntington Dr./Colorado Blvd. arterial corridor in Arcadia, California shown in Figure 5 that is adjacent to Interstate 210. The network comprises 50 links and 13 signalized intersections. Traffic demand and empirical turn ratios were obtained from several sources as part of the Connected Corridors project at UC Berkeley [17].

The signalized intersections operate with fixed-time policies and hence with fixed green splits. In actuality, 11 of the 13 signalized intersections possess a common cycle time of 120 seconds; the remaining two intersections operate with cycle times of 90 seconds and 145 seconds. Our analysis requires a common cycle time for all intersections, and thus we have scaled the fixed green splits for these two intersections so that all signalized intersections operate with a common cycle time of 120 seconds for our study. We refer to this scenario, where phase offsets are obtained from given phase plans, as the *baseline* scenario in Table 4.

Twenty-seven of the 50 links constitute the two-way arterial along Huntington Dr. and Colorado Blvd. to the entry ramp of I-210 along Michillinda Avenue. The remaining links direct exogenous traffic onto the network at intersections and constitute $\mathcal{E}$. The exogenous flows for the two entry links corresponding to the main arterial are 1100 vehicles per hour (vph) and 2000 vph. The exogenous flows for the remaining 21 entry links range from 93 vph to 969 vph with an average of 443 vph. Moreover, the turning ratio of traffic that turns onto the main arterial corridor from other entry links ranges from 7% to 93%, and thus this additional traffic is significant. Therefore, traditional techniques that aim only to maximum the greenband along the arterial, such as [5], are insufficient for this case study. We assume vehicles arrive as a steady stream to all links $\ell \in \mathcal{E}$, that is, $\alpha_\ell = 0$ for all $\ell \in \mathcal{E}$ and thus remove $\mathbf{z}_\epsilon$ from the optimization problem.

We solve (20)–(22) using the MATLAB-based CVX package [27], which returns an optimal $\mathbf{Z}_\star$ in 0.37 seconds on a standard laptop (we could also use CVXOPT, as in the previous case study). As in the previous case study, CVX returned $\mathbf{Z}_\star$ such that $\mathbf{rank}(\mathbf{Z}_\star) = 1$ so that we are able to obtain an exact solution to (16)–(17) with the factorization $\mathbf{Z}_\star = \mathbf{z}_\star(\mathbf{z}_\star)^H$. Unlike the previous case study, we are guaranteed to obtain an optimal $\mathbf{Z}_\star$ that is rank-one because the underlying graph structure is acyclic for which the relaxation has been shown to be exact [23]; as remarked above, when determining the "underlying graph structure", we only consider the existence of a link between a pair of signals and not the direction of travel. In Table 4, we refer to the scenario where phase offsets are the optimized phase offsets as the *optimized* scenario.

To evaluate the performance of the optimized phase offsets, we again simulate the network using the PointQ simulator. Vehicles execute turn movements which are randomly realized according to fixed turn ratios. The simulation is run for a sufficiently long time period so that stochastic fluctuations are negligible.

Results of this simulation are shown in Table 4. We see an improvement of approximately 27% for both the mean peak queue lengths and the mean average queue lengths on links $\mathcal{L}\backslash\mathcal{E}$.

Metric	Baseline	Optimized	Improvement
Mean of Peak Queue Lengths[a,b] [veh]	17.14	12.47	27.2%
Mean of Avg. Queue Lengths[b] [veh]	5.12	3.72	27.4%
Avg. Time in Network [s]	127.9	116.6	8.9%

[a]To account for stochastic fluctuations in the simulation arising from the randomly realized turn rations, the peak queue is defined to be the queue length that is surpassed by the queue process only one percent of the time.

[b]The summation is over $\mathcal{L}\backslash\mathcal{E}$ as noted in Section 6.

Table 4: Results for the Huntington Dr./Colorado Blvd. arterial corridor case study.

7. Conclusions

We have developed a scalable approximation algorithm to the offset optimization problem in arbitrary network topologies. Despite the simplifying assumptions in the problem formulation, the case study simulations demonstrated a significant reduction in the queue lengths. Future work will investigate robust and stochastic generalizations which are important when considering, for example, a distribution of travel times for each link. In addition, a weighted objective function may be used to, *e.g.*, encourage short queues on short links to prevent congestion and is another direction for future research. Additionally, we will consider accommodating different cycle lengths throughout the network. For example, it is natural to consider the case when each cycle time is an integer multiple of some common cycle time. Furthermore, while standard implementations of SDP solvers are able to accommodate on the order of 100 intersections, larger networks require alternative techniques. Future research will apply new algorithms for solving low-rank semidefinite programs and will further study distributed optimization methods such as ADMM [28] that will allow our approach to apply at city-wide scales.

Reducing queue lengths is the explicit performance metric employed in this paper and results in a number of direct benefits (*e.g.*, reduced emissions and likelihood of accidents due to reduced speed oscillations, and reduced "wasted green time" caused by downstream congestion that blocks flow). Reduced queue lengths also afford proximate improvement in other metrics. For example, in the arterial corridor case study, the offset optimization procedure results in decreased travel time of nearly 9% for all vehicles in the network. Future research will further investigate the connection between offset optimization and additional metrics, particularly as it relates to the "bandwidth" maximization problem [5].

[1] R. E. Allsop, "Delay-minimizing settings for fixed-time traffic signals at a single road junction," *IMA Journal of Applied Mathematics*, vol. 8, no. 2, pp. 164–185, 1971.

[2] A. Korsak, "An algorithm for globally-optimal nonlinear-cost multidimensional flows in networks and some special applications," *Operations Research*, vol. 21, no. 1, pp. 225–239, 1973.

[3] Traffic Research Corporation, *SIGOP: Traffic Signal Optimization Program: a Computer Program to Calculate Optimum Coordination in a Grid Network of Synchronized Traffic Signals*. Traffic Research Corp., 1966.

[4] J. Little, M. Kelson, and N. Gartner, "MAXBAND: A versatile program for setting signals on arteries and triangular networks," *Transportation Research Record*, vol. 795, 1981.

[5] G. Gomes, "Bandwidth maximization using vehicle arrival functions," *IEEE Transactions on Intelligent Transportation Systems*, vol. 16, pp. 1977–1988, Aug 2015.

[6] R. E. Allsop, "Selection of offsets to minimize delay to traffic in a network controlled by fixed-time signals," *Transportation Science*, vol. 2, no. 1, pp. 1–13, 1968.

[7] N. Gartner and J. Little, "The generalized combination method for area traffic control," *Transportation Research Record*, pp. 58–69, 1975.

[8] N. Gartner and C. Stamatiadis, "Arterial-based control of traffic flow in urban grid networks," *Mathematical and Computer Modelling*, vol. 35, pp. 657–671, 2002.

[9] N. Gartner and C. Stamatiadis, "Progression optimization featuring arterial and route based priority signal networks," *Journal of Intelligent Transportation Systems: Technology, Planning, and Operations*, vol. 8:2, pp. 77–86, 2004.

[10] N. H. Gartner, J. D. Little, and H. Gabbay, "Optimization of traffic signal settings by mixed-integer linear programming: Part I: The network coordination problem," *Transportation Science*, vol. 9, no. 4, pp. 321–343, 1975.

[11] S. Wong, "Derivatives of performance index for the traffic model from TRANSYT," *Transportation Research B*, vol. 29B, no. 5, pp. 303–327, 1995.

[12] S. Wong, "Group-based optimization of signal timings using the TRANSYT traffic model," *Transportation Research B*, vol. 30, no. 3, pp. 217–244, 1996.

[13] Z.-Q. Luo, W.-K. Ma, A.-C. So, Y. Ye, and S. Zhang, "Semidefinite relaxation of quadratic optimization problems," *Signal Processing Magazine, IEEE*, vol. 27, no. 3, pp. 20–34, 2010.

[14] S. Low, "Convex relaxation of optimal power flow part I: Formulations and equivalence," *IEEE Transactions on Control of Network Systems*, vol. 1, pp. 15–27, March 2014.
[15] A. S. Bandeira, N. Boumal, and A. Singer, "Tightness of the maximum likelihood semidefinite relaxation for angular synchronization," *arXiv preprint, arXiv:1411.3272*, 2014.
[16] A. Singer, "Angular synchronization by eigenvectors and semidefinite programming," *Applied and Computational Harmonic Analysis*, vol. 30, pp. 20–36, 2011.
[17] "Analysis, modeling, and simulation workshop at Caltrans D7." `www.connected-corridors.berkeley.edu/analysis-modeling-and-simulation-workshop-caltrans-d7-0`.
[18] S. Coogan, G. Gomes, E. Kim, M. Arcak, and P. Varaiya, "Offset optimization for a network of signalized intersections via semidefinite relaxation," in *IEEE Conference on Decision and Control*, pp. 2187–2192, 2015.
[19] A. Muralidharan, S. Coogan, C. Flores, and P. Varaiya, "Management of intersections with multi-modal high-resolution data," *Transportation Research Part C*, vol. 68, pp. 101–112, 2016.
[20] A. Muralidharan, R. Pedarsani, and P. Varaiya, "Analysis of fixed-time control," *Transportation Research Part B: Methodological*, vol. 73, no. 0, pp. 81 – 90, 2015.
[21] N. H. Gartner and R. Deshpande, "Harmonic analysis and optimization of traffic signal systems," in *Transportation and Traffic Theory 2009: Golden Jubilee*, pp. 345–364, Springer, 2009.
[22] P. Varaiya, "The max-pressure controller for arbitrary networks of signalized intersections," in *Advances in Dynamic Network Modeling in Complex Transportation Systems*, pp. 27–66, Springer, 2013.
[23] S. Sojoudi and J. Lavaei, "Exactness of semidefinite relaxations for nonlinear optimization problems with underlying graph structure," *SIAM Journal on Optimization*, vol. 24, no. 4, pp. 1746–1778, 2014.
[24] A. M.-C. So, J. Zhang, and Y. Ye, "On approximating complex quadratic optimization problems via semidefinite programming relaxations," *Mathematical Programming*, vol. 110, no. 1, pp. 93–110, 2007.
[25] M. Andersen, J. Dahl, and L. Vandenberghe, "CVXOPT: A python package for convex optimization," 2015. cvxopt.org.
[26] J. Lioris, A. Kurzhanskiy, D. Triantafyllos, and P. Varaiya, "Control experiments for a network of signalized intersections using the '.Q'," *12th IFAC-IEEE Workshop on Discrete Event Systems, Ecole Normale Superieure de Cachan, France*, 2014.
[27] M. Grant and S. Boyd, "CVX: Matlab software for disciplined convex programming, version 2.1." `http://cvxr.com/cvx`, Mar. 2014.
[28] S. Boyd, N. Parikh, E. Chu, B. Peleato, and J. Eckstein, "Distributed optimization and statistical learning via the alternating direction method of multipliers," *Foundations and Trends in Machine Learning*, vol. 3, no. 1, pp. 1–122, 2011.